How cognitive and reactive fear circuits optimize escape decisions in humans

Song Qi[a,b,1], Demis Hassabis[c], Jiayin Sun[b,d], Fangjian Guo[e], Nathaniel Daw[f], and Dean Mobbs[a,1]

[a]Division of the Humanities and Social Sciences, California Institute of Technology, Pasadena, CA 91106; [b]Department of Psychology, Columbia University in the City of New York, New York, NY 10027; [c]Google DeepMind, London N1C 4AG, United Kingdom; [d]School of Humanities and Social Sciences, Harbin Institute of Technology, Heilongjiang 150001, China; [e]Department of Electrical Engineering and Computer Science, Massachusetts Institute of Technology, Cambridge, MA 02139; and [f]Department of Psychology, Princeton University, Princeton, NJ 08544

Edited by Michael S. Gazzaniga, University of California, Santa Barbara, CA, and approved February 8, 2018 (received for review September 6, 2017)

Flight initiation distance (FID), the distance at which an organism flees from an approaching threat, is an ecological metric of cost–benefit functions of escape decisions. We adapted the FID paradigm to investigate how fast- or slow-attacking "virtual predators" constrain escape decisions. We show that rapid escape decisions rely on "reactive fear" circuits in the periaqueductal gray and midcingulate cortex (MCC), while protracted escape decisions, defined by larger buffer zones, were associated with "cognitive fear" circuits, which include posterior cingulate cortex, hippocampus, and the ventromedial prefrontal cortex, circuits implicated in more complex information processing, cognitive avoidance strategies, and behavioral flexibility. Using a Bayesian decision-making model, we further show that optimization of escape decisions under rapid flight were localized to the MCC, a region involved in adaptive motor control, while the hippocampus is implicated in optimizing decisions that update and control slower escape initiation. These results demonstrate an unexplored link between defensive survival circuits and their role in adaptive escape decisions.

fear | anxiety | escape | ecology | decision making

Survival depends on the adaptive capacity to balance fitness-promoting behaviors, such as copulation and foraging, with the omnipresent risk of lethal predatory attack (1, 2). In the field of behavioral ecology, this balance between survival behaviors is depicted by economic models of flight initiation distance (FID), which capture risk functions by measuring the distance at which an organism flees from an approaching threat, while considering the cost of fleeing (1, 3, 4). A wealth of ethological literature demonstrates that prey are remarkably adept at escape and make decisions based on the predator's directionality, lethality, velocity, and previous experience with the predator (5). In addition to its capacity to measure escape decisions, FID is a well-established index of threat sensitivity, resulting in large variability within and between species (5). Despite FID measures being applied to a large variety of taxa, this reliable measure has not been used to identify heterogeneity in threat sensitivity or escape decisions in humans, and the neural circuits remain unexplored.

Theoretical and neuroanatomical models support the existence of an interconnected defensive survival circuitry that is remarkably preserved across species (2, 6–9). Under the conditions of immediate danger, the "reactive fear" circuitry is evoked. This circuitry includes the midbrain periaqueductal gray (PAG), central amygdala (CeA), hypothalamus, and the midcingulate cortex (MCC), which relay, update, and initiate essentially innate reactions including flight and freezing (7, 10–14). Conversely, the ventromedial prefrontal cortex (vmPFC), posterior cingulate cortex (PCC), hippocampus, and basolateral amygdala form a collective set of regions that constitutes the "cognitive fear" circuitry that promotes more complex information processing involved in behavioral flexibility, internal risk assessment, and cognitive avoidance strategies (2, 15–17). Although few behavioral ecologists have considered the neurophysiology underlying escape decisions, some have proposed similar dichotomies suggesting that fast, but inaccurate, decisions are processed by subcortical regions, while slow, but accurate, decisions are processed by cortical system (18, 19). Under natural conditions, both cognitive- and reactive-fear circuits work in harmony by adaptively switching between survival circuits to engage the most optimal strategy to maximize escape (2, 13, 17, 20).

Excitation and inhibition between these circuits is determined by the spatiotemporal distance to the threat (9, 13, 15, 21). For example, distant threat often results in freezing and threat assessment, yet when the threat is close, active flight will be observed (9). Distance to the threat, therefore, is crucial in choosing the best escape strategy. Evidence suggests that this pattern is conserved across various species. In humans, active escape tasks have been used, where the goal of the subject is to escape from a virtual looming threat with the capacity to chase, capture, and shock the subject in a virtual maze. Functional MRI (fMRI) results show that when a threat is distant, there is increased activity in the vmPFC, PCC, and basolateral nucleus of the amygdala. Conversely, as the threat moves closer, there is a switch to increased activity in the CeA and PAG (19, 22, 23). However, these, and related studies, have failed to investigate the neural basis of escape decisions (i.e., flight initiation) or examination the computational mechanisms that underlie escape decisions to changing attack distances.

We developed a paradigm to investigate how the defensive survival circuitry facilitates escape decisions when subjects encounter fast- or slow-attacking threats (Fig. 1*A*). In this task, participants encountered virtual predators of three colors, each representing different attack distances (ADs). On each trial, the

Significance

Humans, like other animals, have evolved a set of neural circuits whose primary function is survival. In the case of predation, these circuits include "reactive fear" circuits involved in fast escape decisions and "cognitive fear" circuits that are involved in more complex processing associated with slow strategic escape. Using neuroimaging combined with computational modeling, we support this differentiation of fear circuits by showing that fast escape decisions are elicited by the periaqueductal gray and midcingulate cortex, regions involved in reactive flight. Conversely, slower escape decisions rely on the hippocampus, posterior cingulate cortex, and prefrontal cortex, a circuit implicated in behavioral flexibility. These results support a separation of fear into reactive and cognitive circuits.

Author contributions: S.Q., D.H., J.S., N.D., and D.M. designed research; S.Q. performed research; S.Q., F.G., N.D., and D.M. analyzed data; and S.Q., D.H., F.G., N.D., and D.M. wrote the paper.

The authors declare no conflict of interest.

This article is a PNAS Direct Submission.

[1]To whom correspondence may be addressed. Email: sqi@caltech.edu or dmobbs@caltech.edu.

This article contains supporting information online at www.pnas.org/lookup/suppl/doi:10.1073/pnas.1712314115/-/DCSupplemental.

Published online March 5, 2018.

actual AD was drawn from a Gaussian distribution that was unique to the particular predator type. Fast-attacking predators (i.e., predators that attack from a larger distance) were characterized by the virtual predator quickly switching from slow approach to fast attack velocity, therefore requiring the subject to make quick escape decisions. On the other hand, slow-attacking predators (i.e., predators that attack from a smaller distance) slowly approached for longer time periods, resulting in larger buffer zones leading to more time to strategize escape. All types of predator loomed and sped up at the same rate, and only differed in their timing of attack.

The goal of the task was to escape from the predator while, at the same time, attempting to acquire as much money as possible by fleeing as late as possible (Fig. 1*B*). Using this task, we proposed several hypotheses: (*i*) for fast escape decisions, we expect to see activity in the reactive fear circuitry, while slow escape decisions will reveal more pronounced activity in the cognitive fear circuitry. In addition, (*ii*) using a Bayesian decision-making model where subjects' preference to reward and avoidance to punishment are considered, we predict that the reactive and cognitive fear circuits will play a corresponding role in facilitating fast and slow escape decisions, respectively.

Results

Behavior. We first examined the behavioral data by applying a repeated-measures, three-way ANOVA (predator type by reward level by shock level) for escape responses (e.g., FIDs). Results showed a main effect of predator type [$F_{(2,54)} = 82.59$, $P < 0.001$]. Post hoc comparisons for the predator type by shock level interaction revealed that the difference in FID choices between high and low shock levels exists only in the slow-attacking predator condition ($P = 0.013$). This shows that subjects took the level of potential danger into consideration while choosing FID (more risk-averse when shock is higher), but only in the slow-attacking threat where there was time for strategic avoidance. The same repeated-measures three-way ANOVA was performed for escape difficulty ratings. A main effect of predator type was found [$F_{(2,54)} = 49.77$, $P < 0.001$], showing that subjects estimate fast-attacking predator as the most difficult predator type to escape (all post hoc comparisons: $P < 0.001$). Significant interactions were found for predator type by shock level [$F_{(2,54)} = 13.68$; $P < 0.001$] and predator type by reward level [$F_{(2,54)} = 4.39$; $P = 0.017$]. For the predator type by shock level interaction, we found that rating was higher in the high shock condition, but only in the slow-attacking predator (post hoc comparison:

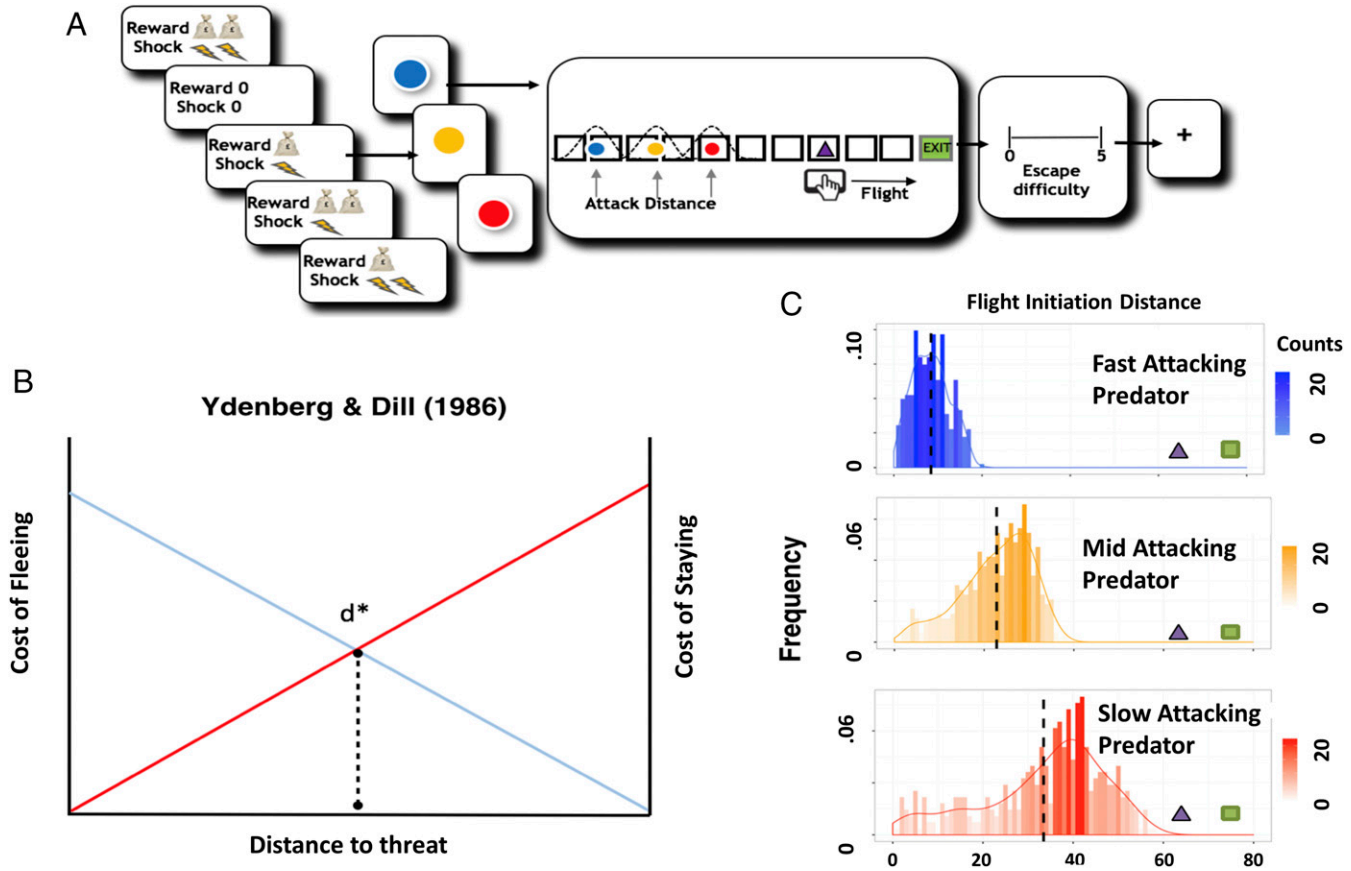

Fig. 1. Experimental procedures, Ydenberg and Dill model (1), and distribution of escape decisions. (*A*) Subjects are told whether their decisions will result in high or low reward or shock. They are then presented with the image of the virtual predator where the color signals the attack distance (2 s) (e.g., blue, fast; red, slow). After a short interval, the virtual predator appears at the end of the runway and slowly moves toward the subject's triangle. After an unspecified amount of time (e.g., 4–10 s), the artificial predator will attack the subject's virtual triangle exit (i.e., attack distance). To escape, the subject must flee before the predator attacks. If the subject is caught, they will receive a tolerable, yet aversive, shock to the back of the hand. Trials end when the predator reaches the subject or the exit. To motivate longer fleeing time, the task will include an economic manipulation, where subjects will obtain more money the longer they stay in the starting position and lose money the earlier they enter the safety exit. After each trial, the subject is asked to report how difficult they found it to escape the virtual predator (4 s). (*B*) Modified schematic representation from the model proposed by Ydenberg and Dill (3). As the distance between the prey and the predator decreases, the cost of fleeing decays, while the cost of not fleeing rises. *D** represents an optimal point where the prey should flee. (*C*) Histograms showing the distribution of subjects' flight initiation decision (FID) choices for early-, mid-, and late-attacking predators, respectively. The x axis represents FID, while the *y* axis represents frequency of choice.

$P < 0.001$). This is intriguing because the predator's attack distance is identical at both shock levels, yet subjects perceived the threat to be more difficult to escape in the high-shock condition (*SI Appendix*, Fig. S1).

Neural Basis of Fast and Slow Escape Decisions. We next investigated the neural basis of the escape decisions for the fast- and slow-attacking threats. To control for timing differences between conditions, besides modeling the rest of the trial as a boxcar function, we specifically looked at the 2 s before the FID button press as a period where subjects form their final decisions. We chose to time lock 2 s before the flight initiation decision for several reasons: (*i*) it allowed us to examine the neural ramping up of the flight initiation, (*ii*) it controlled for the contamination of outcome, and (*iii*) it reduced the amount or trials that would be lost for the fast-attacking condition. Also, to control for any confounds of pain, we excluded the caught trials (number of caught trials: fast-attacking predator, mean, 8 ± 3; mid-attacking predator, mean, 5 ± 2; slow-attacking predator, mean = 4 ± 1), using these events as regressors of no interest. As the mid-attacking condition was a priori used an anchor for the fast- and slow-attacking threats, we focus on activity for the fast and slow attacking. A whole-brain analysis was first performed to locate regions associated with decisions under reactive fear (fast-attacking predators) and cognitive fear (slow-attacking predators). Detailed regions of activation can be found in *SI Appendix*, Tables S1 and S2. As shown in Fig. 2, data extracted from a priori and independent anatomical regions of interest (ROIs) of PAG, MCC, PCC, hippocampus, and vmPFC, were differentially activated for the different predator conditions.

To confirm the dissociation between the reactive and cognitive fear systems (represented by PAG and vmPFC, respectively), we computed a two-way ANOVA (region by predator type) using signal change drawn from independent ROIs from PAG and vmPFC. There was a main effect of region ($F = 5.77$, $P = 0.017$) and a significant interaction between region and predator type ($F = 11.50$, $P < 0.001$). For the [fast-attacking predator > control] contrast, we observed increased activity in PAG and MCC. A direct comparison between high and low shock levels for the fast-attacking predator revealed increased activity in the PAG, suggesting that PAG is evoked when the threat is high (*SI Appendix*, Table S7).

On the other hand, the [slow-attacking predator > control] contrast revealed increased activity in the cognitive fear circuitry including the vmPFC, PCC, and the hippocampus. While no amygdala was observed for the main contrast, a direct comparison between high and low shock levels in the slow-attacking predator condition showed increased activity in the amygdala and hippocampus (*SI Appendix*, Table S8). To further disentangle the effect and increase the sensitivity of the analysis, we extracted the signal changes and BOLD-signal time series from the predefined ROIs (i.e., PAG, MCC, vmPFC, PCC, and hippocampus), regions that have previously been associated with fear, anxiety, and decision making under stress (22). A conjunction between fast- and slow-attacking threats showed that the medial dorsal thalamus (MDT) was commonly activated. Although this is an exploratory finding, it is intriguing because MDT is directly or indirectly connected to both fear circuits, since stimulation of the MDT results in depression or potentiation of both circuits and it is thought to play a role in behavioral flexibility (24, 25).

Computations That Support Escape Decisions. To explore how the observed FIDs might be understood in terms of rational decision making (i.e., the costs and benefits of flight), we developed a Bayesian decision-making model. The process by which subjects make escape choices under different predator ADs can be decomposed to two steps: (*i*) predicting predators' distribution of attack distances, by learning from experience; and (*ii*) choosing an FID by comparing the money that can be possibly obtained against the potential risk of shock for each possible FID, in expectation over the predicted attack distance distribution and informed by the individual's subjective preference levels for shock vs. money. We assume a Bayesian ideal observer model of subjects' learning to estimate the attack distances of different predators from trial-by-trial experience. FID choices are then determined (with softmax noise) by computing the expected utility for each possible escape distance. We then calculated the distance between utility resulted from subjects' actual FID and the predicted Bayes ideal FID, which is considered a measure of optimal performance. The modeling results are shown in Fig. 3 and *SI Appendix*, Figs. S3 and S4. Details of the model are explained in *SI Appendix*, *SI Text*.

We next examined the neural circuits that correlated with each subjects' preference parameters in the Bayesian decision model. For a rational player, the preference for reward should be positive, while the preference for shock should be negative. Thus, greater reward or shock sensitivity here corresponds to larger (positive) β_2 and smaller (negative) β_1 amplitudes. The parametric modulation analysis over the [predator > control] contrasts revealed that, for the fast-attacking predator condition, higher reward sensitivity was associated with activations in

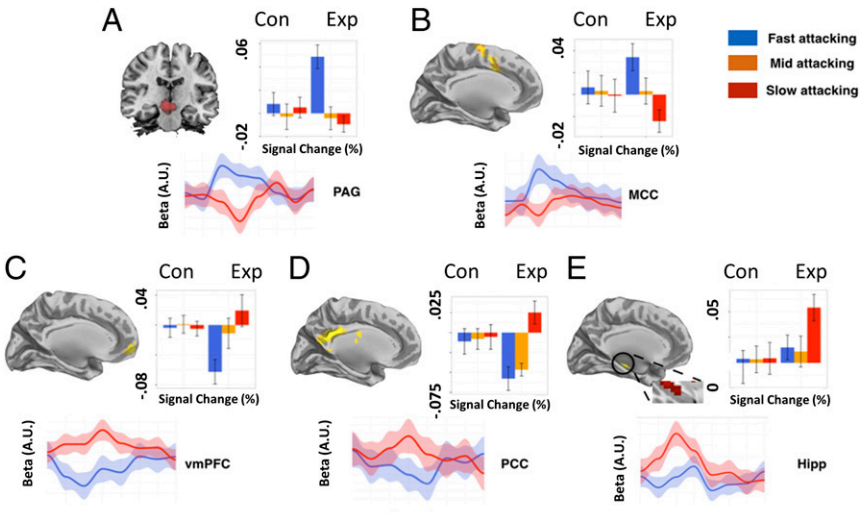

Fig. 2. Main regions of interest and signal changes associated with fast- and slower-attacking threats. Parameter estimates and time series extracted from (*A*) midbrain, (*B*) MCC, (*C*) vmPFC, (*D*) PCC, and (*E*) the hippocampus. Activations shown in the graph show clusters from the whole-brain activation, while the signal change data were extracted from independent anatomical ROIs. The *Upper* graph displays parameter estimates. The *y* axis represents percent signal changes, and the *x* axis is the predator type. The *Lower* graph display time series extracted in a course of 16 s. Blue line: fast predator; red line: slow predator. The beginning of the time series represents the time point when the FID event comes online.

bilateral putamen, while higher shock sensitivity is associated with engagement in PAG and bilateral insula. On the other hand, for the slow-attacking predator condition, right caudate was found to be associated with higher reward sensitivity, while PCC was found to be associated with higher shock sensitivity. A display of the activated regions can be found in *SI Appendix*, Fig. S3. A detailed layout of the activated regions can be found in *SI Appendix*, Tables S9 and S10.

Next, to investigate what neural circuits are responsible for the optimization of escape decisions, we considered a measure of performance optimality related to the per-trial spread between subjects' actual and Bayesian ideal FIDs. In particular, we computed the difference between the actual trial-specific utility $U(FID)$ and the maximum (Bayes optimal) utility the subject could possibly get on the trial $[U(FID)_{max}]$, given their estimated subjective utilities. A smaller difference (e.g., less regret relative to ideal) implies more consistent Bayesian decision making; variation around the ideal FID will increase the difference. The differences on every trial were entered as a subject-level parametric modulator separately under each [predator > control] conditions. For the fast-attacking predator condition, we found that better Bayesian decisions (smaller distance to ideal) was associated with activity in MCC, middle frontal gyrus, and superior motor cortex. On the other hand, better Bayesian decision making in the slow-attacking predator condition was found to be associated with activity in bilateral hippocampus, as shown in Fig. 4.

Functional Connectivity Between Computationally Defined Regions. To investigate the interplay among the brain regions involved in escape decision optimization, a functional connectivity analysis was performed for the response phase (escape decision) using a generalized psychophysiological interactions approach (26); to confirm the patterns observed in the whole-brain flexible model, we first adopted independent seed regions of MCC and hippocampus from previous research (19). For the contrast of [fast-attacking predator > control], we showed a significant coupling between the MCC seed, the PAG, motor cortex, and bilateral thalamus. For the contrast of slow predator > control, we showed a significant coupling between the hippocampus seed and PCC. This suggests that, when the subjects are provided time for decision flexibility, they use a search-and-employ approach that prepares them for action, as shown in Fig. 4.

Discussion

We have demonstrated that subjects apply different nodes of the survival circuitry when escaping fast- and slow-attacking threats. Our analysis revealed increased activity in reactive-fear circuits, namely the PAG and the MCC for the fast attacking predator, regions that are implicated in motor response to fast and imminent threats. Supporting comparative work (27), connectivity analysis revealed a significant couple between the MCC and PAG. Recent animal work has also shown the optogenetic activation of glutamatergic neurons in the dorsal lateral PAG induce motor responses [e.g., flight (11)]. The MCC is also a critical component of the defensive survival circuitry and has afferent projections to the ventral striatum, receives efferent signals from the medial dorsal thalamus, and has bidirectional projections with the amygdala (10). It has also been suggested that control signals in the MCC may resolve conflict between defensive strategies (e.g., freezing or fleeing). This has led to the theory that the cells in the MCC are involved in linking motor centers with defensive circuits (10).

Our analysis for the slow-attacking threat contrast revealed activation in three key areas of the cognitive fear circuitry involved in more complex information processing—the vmPFC, hippocampus, and PCC. Structural and function connectivity between these structures has been shown in humans and primates, supporting conserved pathways across species (8). Primate research has found that the primate PCC responds to risky decision making and scales with the degree of risk (28). The PCC is also correlated with a salience signal reflecting the deviation from the standard option, suggesting a role in the flexible allocation of neural resources (29). A function of the PCC may be to harvest information for escape decisions under conditions of protracted threat. This fits with the proposal that, through its connections with the hippocampus, the PCC may integrate memory guided decisions with current decision processes that may involve a "preparation for action" by anticipating and altering behavioral policies (30).

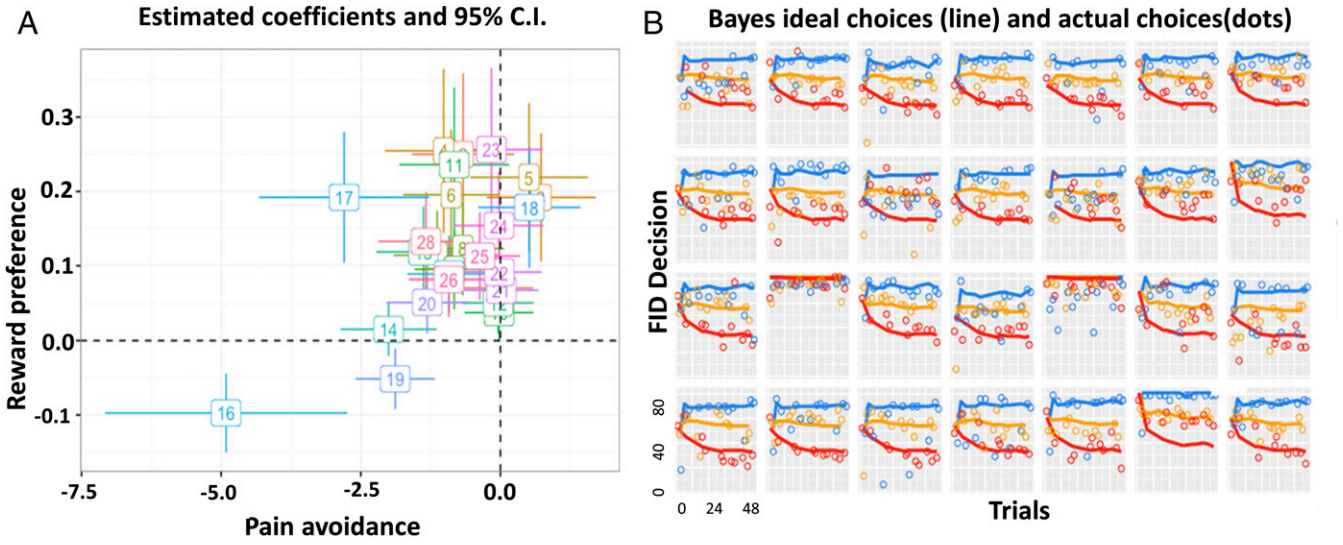

Fig. 3. Visualization of Bayesian modeling results. (*A*) Estimated coefficients for each subject for the first scanning session, along with 95% confidence intervals. The *x* axis represents the pain coefficient β_1 in the utility function, and the *y* axis represents the monetary reward coefficient β_2. For a rational player, β_2 should be positive (seeking money), and β_1 should be negative (avoiding shock). (*B*) Model fit to observed FIDs for the first scanning session. The *x* axis represents trial numbers, and the *y* axis represents FID. Ideal FID choices predicted by the ideal Bayesian observer (lines), subjects' actual FID choice (dots). Average values of reward preference and shock avoidance of the two scanning sessions were used as parametric modulators for the fMRI analysis. Data for session 2 can be found in *SI Appendix*, Fig. S4.

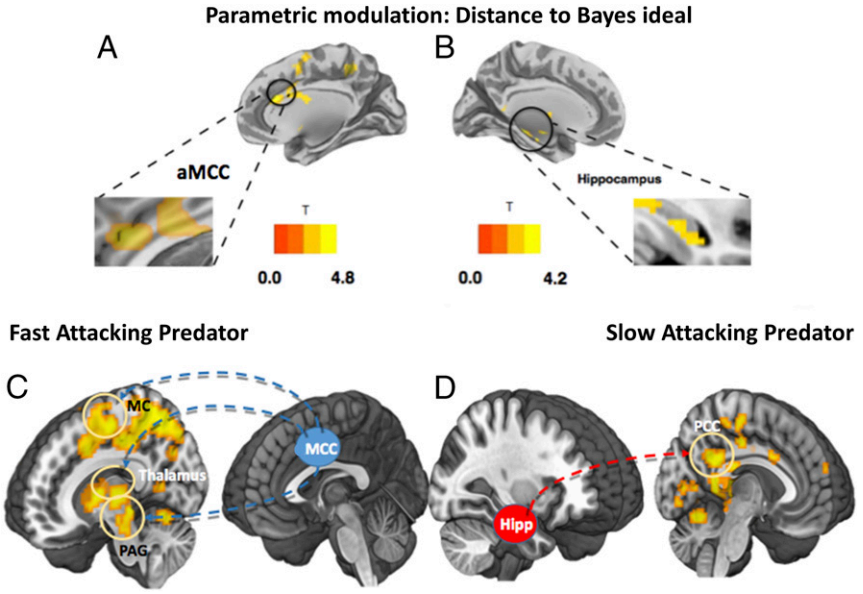

Fig. 4. Regions, and their connectivity, associated with parametric modulation of "distance to ideal." (*A*) Brain regions associated with increased Bayesian decision optimality in the fast AD condition. Better decision making was associated with increased activity in MCC and superior motor cortex. (*B*) Brain regions associated with decreased distance (increased Bayesian decision optimality) in the slow AD condition activated regions include bilateral hippocampus and bilateral caudate. A display of the correlation results can be found in *SI Appendix*, Table S11. (*C*) Connectivity analysis using MCC as seed over the contrast [fast predator > control]. Positive connectivity was found between MCC, motor cortex (MC), thalamus, and the PAG. (*D*) Using the hippocampus as seed over the contrast [slow predator > control], positive connectivity was found between the hippocampus and PCC.

The vmPFC is also a key player in the defensive survival circuitry. Single-cell recordings in rodents have shown that the mPFC contains "strategy-selective" cells, which are thought to be involved in the coordination of defensive responses (21). This fits with the idea that the mPFC plays a role in selecting adaptive strategies that are mapped onto motor responses. Indeed, work in humans shows that larger buffer distances are associated with activity in the vmPFC, and decreased activity in these regions is associated with panic-related motor actions (22, 23, 31). Our data build on these findings by showing that the vmPFC, hippocampus, and PCC form a strategic and flexible decision process (17, 32), when the agent has time to contemplate the best escape action. Our findings tentatively support the role of complex cortical information processing circuits (i.e., cognitive fear circuits) in "slower" escape decisions associated with flexible and strategic avoidance through internal risk assessment that involve model-based memory search (16, 33). This fits with a model-based perspective where actions are deliberative and employ a cognitive-style representation, which is an internal map of events and stimuli from the external world, and take prospective assessment of the consequences of an action (34). Thus, the cortical activity observed here could represent "reflective computations" associated with higher information processing and cognitive architecture (30).

Our Bayesian model also provides insights into how the distinct regions of the survival circuits associated with optimal escape. Two core regions were associated with optimal escape: the MCC for the fast-attacking threat and the hippocampus for the slow-attacking threat. While it is accepted that the PAG needs input to make optimal decisions, it is unclear where this input comes from. A few candidates exist; among them is the MCC. The MCC is highly connected to the lateral PAG and according to adaptive control theory is a "central hub" where information about reinforcers are passed to motor control areas to coordinate goal-directed behaviors (10). Our connectivity results support this conclusion showing that the MCC was coupled with activity in the PAG and the motor cortex. This proposes that the MCC is one candidate region for the integration of current goals and implement aversively motivated instrumental motor behaviors [i.e., when to flee a threat (10)].

Theorists have proposed that the hippocampus computes comparators that assess multiple goals and in turn corrects actions (35) possibly through a flexible constructive process involved in problem solving (36) and predictive mapping. When there is time to gather information, the hippocampus may play a role in drawing on previous threat encounters to form a predictive map and optimize current actions (37). The hippocampus also plays a role in spatial and temporal "where" and "when" memory and has theoretically been linked to escape decisions (38) and may act to resolve conflict between fitness-promoting behaviors (1, 3, 4, 39–42). Our computational analysis also revealed a Bayesian role for the hippocampus, where it potentially gathers information to optimize directed escape during slow-attacking, but not fast-attacking, threat. Our connectivity analysis did not reveal connections between these regions but did show that the hippocampus was also coupled with activity in the PCC, a region thought to be involved in adaptive decisions (30).

In summary, we introduce a paradigm that allows researchers to map escape decisions onto the defensive survival circuitry. This circuit can be separated into a fast reactive-fear circuit involved in escape decision when time is limited and a slower cognitive-fear circuit that is involved in more complex information processing associated with the strategic avoidance and flexible escape decisions. More specifically, sections of these circuits differentially optimize escape decisions with the MCC centered on making fast decisions associated with imminent threat and the hippocampus in slow strategic decisions that are characterized by protracted threat assessment. These results provide a window in the role of the defensive survival circuitry in adaptive escape decisions and transform the way we view the neural circuits involved in human fear. Clearly, more work needs to be conducted to validate the reactive and cognitive distinction of fear. Future interventions using pharmacological agents and noninvasive methods (e.g., transcranial magnetic stimulation) could be used to examine more causal functions of these fear circuits and how they manifest in changes in computational strategies.

Methods

Participants. A total number of 30 subjects completed informed consent in accordance with the guidelines of the Columbia University IRB and were remunerated for their participation. Data from one subject were lost due to computer error. One additional subject was excluded due to excessive movement during the scan. Our final sample consisted of 28 subjects (17 women; age, 25.4 ± 7.3 y).

Experiment Design. Subjects were scanned while they viewed stimuli on a screen that displayed a 2D runway, with a virtual predator "attacking" from

the left entrance. In the current paradigm, the goal of the subject was to escape the attack from a certain virtual predator, by pressing a button at the desired timing. Once the button was pressed, a triangle representing the subject started moving toward a "safety exit." Subjects gained reward if they escaped to the safety before the predator caught them; on the other hand, they were given a mildly aversive electric shock if they were caught. The key was to choose the right timing to flee: acquire the maximum amount of reward while still escaping the virtual predator. Reward in each trial linearly scaled with time spent before pressing the button. The longer subjects stayed in the starting position (the smaller the FID), the more reward they got. However, if the subjects stayed for too long, they can get caught, which would result in both a loss of all reward for the current trial and the administration of an electric shock. However, they still maintain the cumulative reward they received from previous trials.

The runway has a total length of 90 units, where the subject's triangle is placed 10 units to the safety exit. While in the approaching mode, the predator oscillates toward the subject's triangle at a speed of 4 units/s; while in the chasing mode, the predator proceeds with a speed of 10 units/s. There are 96 trials, factorially divided to cover different predator attack distances, shock level, and reward levels [$3 \times 3 \times 3$; three types of predators; three levels of shock (0, low, and high levels shock); and three levels of reward (0, low, and high levels of reward)]. In the high-shock condition, subjects receive two shocks instead of one. In addition, in the high-reward condition, subjects receive twice the original reward if they escape. The control condition was the zero-reward and zero-shock condition. Subjects were first presented with a screen indicating which type of predator and shock/reward level will be presented in the next trial for 2 s. This shock/reward indicator informs the next four trials. Next, the trial begins, where subjects observe an artificial predator slowly looming toward the triangle representing themselves. After a designated time period, which is learned by the participant, the artificial predator will attack by speeding up when it reaches the attacking position. To make sure reaction time plays no role in FIDs, we manipulated the speed of the predator and the subject so that, once the threat speeds up to attack, it is impossible to escape after that time point. After the trial, subjects are required to rate the difficulty of escape using a visual analog (1–5) scale.

After the first 48 trials, the assignment of predator–color relationship was altered to introduce novelty and avoid the (habitual) fixation of subject strategies. Same colors were reassigned among the predators (e.g., the original fast-attacking predator changes color from blue to red).

Before the start of the actual experiment, subjects went through a brief practice session of eight trials to familiarize themselves with the paradigm. In the practice session, subjects played the same game, but the predators' attack distances were drawn from different distributions other than the ones used in the actual experiment. The level of the electric shock was calibrated according to subjects' level of tolerance (self-reported to be aversive, yet not painful). With a 1–10 scale, the average calibrated shock level was 6.4 (mean, 6.4; SD, 1.3).

Behavioral Analysis. Due to the relative simplicity of our task and exposure to a practice session, subjects' performance reached saturation very quickly after the beginning of the experiment. By "saturation," subjects quickly formed their own patterns of choice making and carry through the rest of the experiment. Thus, instead of looking at trial-by-trial changes of the FID, we focus on the differences of FID between different predator conditions, and approaches subjects' learning behavior by a Bayesian decision-making model.

Subjects' choice of FID, reward from the trial, and escapability ratings were collected on each trial. We used repeated-measures three-way ANOVAs (of predator type by reward level by shock level) to assess differences in FID, reward, and escapability ratings between the various conditions.

The analysis of fMRI data and Bayesian decision-making model can be found in *SI Appendix, SI Text*.

ACKNOWLEDGMENTS. We thank John O'Doherty, Peter Dayan, Alex Shackman, James Curley, and Joe LeDoux for their advice and Nir Jacoby for his work on an earlier version of the paradigm. This study was supported by a grant from National Alliance for Research on Schizophrenia and Depression (to D.M.).

1. Cooper WE, Jr, Blumstein DT, eds (2015) *Escaping from Predators: An Integrative View of Escape Decisions* (Cambridge Univ Press, Cambridge, UK).
2. Mobbs D, Kim JJ (2015) Neuroethological studies of fear, anxiety, and risky decision-making in rodents and humans. *Curr Opin Behav Sci* 5:8–15.
3. Ydenberg RC, Dill LM (1986) The economics of fleeing from predators. *Adv Stud Behav* 16:229–249.
4. Fanselow MS, Lester LS (1988) A functional behavioristic approach to aversively motivated behavior: Predatory imminence as a determinant of the topography of defensive behavior. *Evolution and Learning*, eds Bolles RC, Beecher MD (Lawrence Erlbaum Associates, Hillsdale, NJ), pp 185–212. Available at psycnet.apa.org/record/1987-98812-010. Accessed January 23, 2017.
5. Stankowich T, Blumstein DT (2005) Fear in animals: A meta-analysis and review of risk assessment. *Proc Biol Sci* 272:2627–2634.
6. Panksepp J (1998) The periconscious substrates of consciousness: Affective states and the evolutionary origins of the self. Available at www.ingentaconnect.com/content/imp/jcs/1998/00000005/F0020005/895. Accessed January 4, 2017.
7. Panksepp J (2011) The basic emotional circuits of mammalian brains: Do animals have affective lives? *Neurosci Biobehav Rev* 35:1791–1804.
8. Price JL (2005) Free will versus survival: Brain systems that underlie intrinsic constraints on behavior. *J Comp Neurol* 493:132–139.
9. Blanchard RJ, Blanchard DC (1990) An ethoexperimental analysis of defense, fear, and anxiety. *Otago Conference Series, No. 1. Anxiety*, eds McNaughton N, Andrews G (University of Otago Press, Dunedin, New Zealand), pp 124–133. Available at psycnet.apa.org/record/1990-98566-013. Accessed January 23, 2017.
10. Shackman AJ, et al. (2011) The integration of negative affect, pain and cognitive control in the cingulate cortex. *Nat Rev Neurosci* 12:154–167.
11. Tovote P, et al. (2016) Midbrain circuits for defensive behaviour. *Nature* 534:206–212.
12. LeDoux J (2012) Rethinking the emotional brain. *Neuron* 73:653–676.
13. Mobbs D, Hagan CC, Dalgleish T, Silston B, Prévost C (2015) The ecology of human fear: Survival optimization and the nervous system. *Front Neurosci* 9:55.
14. Gross CT, Canteras NS (2012) The many paths to fear. *Nat Rev Neurosci* 13:651–658.
15. McNaughton N, Corr PJ (2004) A two-dimensional neuropsychology of defense: Fear/anxiety and defensive distance. *Neurosci Biobehav Rev* 28:285–305.
16. McNaughton N, Corr PJ, Survival circuits and risk assessment. *Curr Opin Behav Sci*, in press.
17. Davis M, Walker DL, Miles L, Grillon C (2010) Phasic vs sustained fear in rats and humans: Role of the extended amygdala in fear vs anxiety. *Neuropsychopharmacology* 35:105–135.
18. Trimmer PC, et al. (2008) Mammalian choices: Combining fast-but-inaccurate and slow-but-accurate decision-making systems. *Proc Biol Sci* 275:2353–2361.
19. Mobbs D, et al. (2007) When fear is near: Threat imminence elicits prefrontal-periaqueductal gray shifts in humans. *Science* 317:1079–1083.
20. Amat J, et al. (2005) Medial prefrontal cortex determines how stressor controllability affects behavior and dorsal raphe nucleus. *Nat Neurosci* 8:365–371.
21. Halladay LR, Blair HT (2015) Distinct ensembles of medial prefrontal cortex neurons are activated by threatening stimuli that elicit excitation vs. inhibition of movement. *J Neurophysiol* 114:793–807.
22. Mobbs D, et al. (2009) From threat to fear: The neural organization of defensive fear systems in humans. *J Neurosci* 29:12236–12243.
23. Mobbs D, et al. (2010) Neural activity associated with monitoring the oscillating threat value of a tarantula. *Proc Natl Acad Sci USA* 107:20582–20586.
24. Vertes RP, Linley SB, Groenewegen HJ, Witter MP (2015) Thalamus. *The Rat Nervous System*, ed Paxinos G (Academic, San Diego), 4th Ed, pp 335–390.
25. Krout KE, Loewy AD (2000) Periaqueductal gray matter projections to midline and intralaminar thalamic nuclei of the rat. *J Comp Neurol* 424:111–141.
26. McLaren DG, Ries ML, Xu G, Johnson SC (2012) A generalized form of context-dependent psychophysiological interactions (gPPI): A comparison to standard approaches. *Neuroimage* 61:1277–1286.
27. An X, Bandler R, Ongür D, Price JL (1998) Prefrontal cortical projections to longitudinal columns in the midbrain periaqueductal gray in macaque monkeys. *J Comp Neurol* 401:455–479.
28. McCoy AN, Platt ML (2005) Risk-sensitive neurons in macaque posterior cingulate cortex. *Nat Neurosci* 8:1220–1227.
29. Heilbronner SR, Hayden BY, Platt ML (2011) Decision salience signals in posterior cingulate cortex. *Front Neurosci* 5:55.
30. Pearson JM, Heilbronner SR, Barack DL, Hayden BY, Platt ML (2011) Posterior cingulate cortex: Adapting behavior to a changing world. *Trends Cogn Sci* 15:143–151.
31. Perkins AM, Arnone D, Smallwood J, Mobbs D (2015) Thinking too much: Self-generated thought as the engine of neuroticism. *Trends Cogn Sci* 19:492–498.
32. Moscarello JM, Maren S (2018) Flexibility in the face of fear: Hippocampal-prefrontal regulation of fear and avoidance. *Curr Opin Behav Sci* 19:44–49.
33. LeDoux JE, Pine DS (2016) Using neuroscience to help understand fear and anxiety: A two-system framework. *Am J Psychiatry* 173:1083–1093.
34. Daw ND, Niv Y, Dayan P (2005) Uncertainty-based competition between prefrontal and dorsolateral striatal systems for behavioral control. *Nat Neurosci* 8:1704–1711.
35. McNaughton N, Gray JA (2000) Anxiolytic action on the behavioural inhibition system implies multiple types of arousal contribute to anxiety. *J Affect Disord* 61:161–176.
36. Hassabis D, Maguire EA (2007) Deconstructing episodic memory with construction. *Trends Cogn Sci* 11:299–306.
37. Stachenfeld KL, Botvinick MM, Gershman SJ (2017) The hippocampus as a predictive map. *Nat Neurosci* 20:1643–1653.
38. Litvin Y, Blanchard DC, Blanchard RJ (2015) The physiology of escape. *Escaping From Predators*, eds Cooper WE, Jr, Blumstein DT (Cambridge Univ Press, Cambridge, UK), pp 343–359.
39. Bach DR, et al. (2014) Human hippocampus arbitrates approach-avoidance conflict. *Curr Biol* 24:541–547.
40. Genovese CR, Lazar NA, Nichols T (2002) Thresholding of statistical maps in functional neuroimaging using the false discovery rate. *Neuroimage* 15:870–878.
41. Tedeschi E, Weber J, Prévost C, Mischel W, Mobbs D (2015) Inferences of others' competence reduces anticipation of pain when under threat. *J Cogn Neurosci* 27:2071–2078.
42. Train KE (2009) *Discrete Choice Methods with Simulation* (Cambridge Univ Press, Cambridge, UK), 2nd Ed.